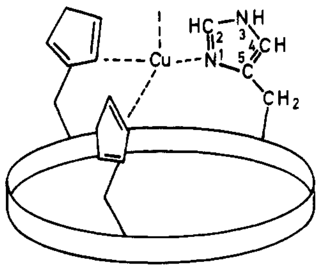

**Figure 6.** Proposed structure of the Cu(II)-G4H3 complex at neutral pH.

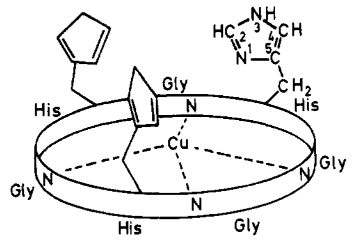

**Figure 7.** Proposed structure of the Cu(II)-G4H3 complex at basic pH.

determine the geometry of Cu(II) complexes in solution.[35] Unfortunately, as pointed out by Espersen and Martin,[27] a large difference between the spin-lattice relaxation time ($T_{1M}$) and the transverse relaxation time ($T_{2M}$) is not unexpected for copper complexes ($T_{1M} \gg T_{2M}$), indicating in the $T_{2M}$ relation an important contribution from the scalar term, which is not distance-dependent. Our results[23,32] and those of many others[22,36] agree well with this assumption. Consequently, selective broadening experiments may not reflect the explicit $r^{-6}$ distance dependence of the dipolar term, even though they may still be used to determine the sites of Cu(II) binding.

On the basis of these observations, it will be interesting to know what the predominant factor is that controls the line broadening in our 1:1 complex. Our first results obtained by measuring the relaxation parameters show that the values of $T_{1M}/T_{2M}$ ratios are less than 2. Consequently, the measured $T_{2M}$ values are largely determined by the dipolar term, implying therefore the possibility of the determination of the copper-nuclei distances.[37] If such major findings are confirmed, they should provide an important contribution to the knowledge of NMR spectroscopy of paramagnetic Cu(II) complexes of biological molecules.

## Concluding Remarks

The following are the main conclusions drawn from the present studies:

(1) The NMR, EPR, and visible spectral data presented herein give direct evidence that, in aqueous solution, the Cu(II) ion interacts with G4H3 to give two kinds of complexes depending on the pH. Around neutral pH, binding occurs through the three N(1) imidazole residues (Figure 6), whereas at basic pH Cu(II) binds via four Gly NH deprotonated peptide nitrogens (Figure 7).

(2) The NMR investigation gives evidence that both complexes are in "slow exchange" conditions, contrary to the general assumption of "fast exchange" in such systems.

(3) A major finding concerns the unusual behavior of G4H3-bound Cu(II) at basic pH, which reveals for the first time the observation of the NMR spectra for a 1:1 Cu(II) complex with this kind of ligand. This phenomenon suggests that Cu(II) is very tightly bound in the cyclic cavity and forms an anomalous long-lived complex.

(4) Unlike the general features underlying the paramagnetic line-broadening properties of Cu(II), our relaxation parameters seem to indicate the predominance of the dipolar term in the $T_{2M}$ relation. Consequently, and for the first time to date, it appears that the $^{1}$H and $^{13}$C NMR technique will be very useful for obtaining structural information about such complexes in solution. These results raise some important questions in relation to the interpretation of the NMR data of paramagnetic Cu(II) complexes in solution made by several authors.

**Acknowledgment.** The research was supported by the Medical Research Council (Canada) and le Centre National de la Recherche Scientifique (France).

---

(35) Ihnat, M. *Biochemistry* **1972**, *11*, 3483-3492.

(36) Gairin, J. E.; Mazarguil, H.; Sharrock, P.; Haran, R. *Inorg. Chem.* **1982**, *21*, 1846-1854.

(37) Laussac, J.-P.; Sarkar, B., unpublished results.

---

Contribution from the Central Salt and
Marine Chemicals Research Institute, Bhavnagar 364002, India

# Oxygen Atom Transfer in the Oxidation of Triphenylphosphine by Molecular Oxygen Catalyzed by an Ru(III)-EDTA-PPh$_3$ Complex

M. M. Taqui Khan,* M. R. H. Siddiqui, Amjad Hussain, and M. A. Moiz

*Received May 23, 1985*

The oxidation of PPh$_3$ to OPPh$_3$ in the presence of Ru(III)-EDTA, PPh$_3$ (1:10), and molecular oxygen in 50% dioxane-water proceeds through the formation of intermediate complexes $[Ru^{III}(EDTA)(H_2O)]$ (**1**), mixed-ligand $[Ru^{III}(EDTA)(PPh_3)]$ (**2**), and the ($\mu$-peroxo)ruthenium(IV) complex $[Ru^{IV}(EDTA)(PPh_3)]_2O_2$ (**3**). The formation of complexes **1**-**3** has been supported by potentiometric, spectrophotometric, electrochemical, and kinetic measurements. The rate of oxidation of PPh$_3$ is first order with respect to Ru(III)-EDTA complex, first order with respect to PPh$_3$ and one-half order with respect to molecular oxygen, thus supporting the formation of **3** as an intermediate in the oxygenation reaction of PPh$_3$. The proposed rate-determining step in the oxidation of PPh$_3$ is the formation of an intermediate ruthenyl complex species $[Ru^{V}{=}O(EDTA)(PPh_3)]$ (**4**) followed by a fast inner-sphere transfer of oxygen atom from **4** to PPh$_3$ to form OPPh$_3$ and the regeneration of $[Ru^{III}(EDTA)(H_2O)]$ (**1**). The system represents an example of a truly catalytic Ru(III) oxygen atom transfer system with a simple non-porphyrinic ligand and molecular oxygen as the oxidant.

## Introduction

The oxidation of triphenylphosphine to triphenylphosphine oxide has attracted much interest in recent years due to its relevance to oxygen atom transfer reactions catalyzed by cytochrome P-450 oxidase.[1-3] A number of oxygen atom transfer reactions to various substrates were reported with Fe(III) ion[4] and Fe(III) porphyrins.[5-12] In these reactions the catalytically active $Fe^{IV}{=}O$ species

---

(1) Collman, J. P.; Groh, S. C. *J. Am. Chem. Soc.* **1982**, *104*, 1391.

(2) Groves, J. T.; McLusky, G. A.; White, R. E.; Coon, M. J. *Biochem. Biophys. Res. Commun.* **1978**, *81*, 154.

(3) Groves, J. T.; Subramanian, D. V. *J. Am. Chem. Soc.* **1984**, *106*, 2177.

(4) Groves, J. T.; Van Derpuy, M. *J. Am. Chem. Soc.* **1976**, *98*, 5290.

(5) Groves, J. T.; Meyers, R. S. *J. Am. Chem. Soc.* **1983**, *105*, 5791.

0020-1669/86/1325-2765$01.50/0 © 1986 American Chemical Society

is generated by the oxidants hydrogen peroxide,[4] iodosylbenzene,[5–10] peroxy acids,[11] and amine oxides.[12] Similar reactivity was reported in manganese and chromium porphyrins.[13–15] Bleomycin-coordinated Mn(III) and Cu(II) ions also take part in the oxygen atom transfer reaction in the presence of iodosylbenzene as an oxidant.[16,17] In these systems[17] iodosylbenzene can be replaced by molecular oxygen in the presence of ascorbic acid. Manganese, iron, and cobalt salts in acetonitrile also catalyze the oxygenation of organic substrates by iodosylbenzene.[18,19] Manganese(III) porphyrins catalyze the epoxidation[20,21] of olefins in the presence of hypochlorite.

Of the heavier transition-metal ions, the oxoruthenium(IV) species $Ru^{IV}{=}O(py)(bpy)$ was used[22] in the noncatalytic oxygen atom transfer to $PPh_3$. The complex Ru(III)–octaethylporphyrin–$PPh_3$ was reported[23] to catalyze the oxygenation of $PPh_3$ by idosylbenzene. Of recent interest are the oxo transfer reaction from $Me_2SO$ to $PPh_3$ catalyzed by molybdyl complexes of the composition $Mo^{VI}O_2(L)$ and $Mo^{IV}O(L)(DMF)$ (L = 2,6-bis-(2,2-diphenyl-2-mercaptoethyl)pyridine) in DMF solution.[24]

Oxidation of triphenylphosphine to a phosphine oxide by molecular oxygen catalyzed by $Ru(SCN)(NO)(PPh_3)_2$ was studied by Graham et al.[25,26] In the catalytic oxidation of $PPh_3$ by $Pt(PPh_3)_2O_2$ an outer-sphere free-radical oxidation of $PPh_3$ by $HO_2^-$ was suggested.[27] Molybdyl complexes of the composition $MoO_2L_2$ (L = $S_2CNR_2$, $S_2PR_2$ (R = Me, Et, *n*-Pr), cysteinato methyl ester, acetylacetonato, 8-hydroxyquinolinato) also catalyze[28,29] the oxidation of $PPh_3$ to phosphine oxide by molecular oxygen. Recently Groves and Quinn[30] reported the catalysis of the Ru(VI) dioxo complex $Ru(TMP)(O)_2$ (TMP = tetramesitylporphyrinato) in the epoxidation of cyclooctene, *cis*-$\beta$-methylstyrene and norbornene by molecular oxygen. A large amount of the catalyst was reported[30] to be converted during the reaction to an unstable paramagnetic ruthenium porphyrin complex.

In the wealth of data available to date on the catalytic oxygenation by metal ions of groups 3d, 4d and 5d (3, 4, and 5[47]), the oxidants are restricted to some organic oxygen transfer agents as cited earlier.[1–24] Catalytic oxygen atom transfer reactions in the presence of molecular oxygen have been studied[25–30] only in a few cases. In the present paper, we report[31] a truly catalytic oxygen atom transfer reaction from molecular oxygen to $PPh_3$ catalyzed by the simple non-porphyrinic $[Ru^{III}(EDTA)(H_2O)]$ complex (**1**) in solution. The reaction proceeds through the formation of the intermediate complex $[Ru^{III}(EDTA)(PPh_3)]$ (**2**) and the ($\mu$-peroxo)ruthenium(IV) intermediate species $[Ru^{IV}(EDTA)(PPh_3)]_2O_2$ (**3**), which were characterized by equilibrium, spectrophotometric, and electrochemical techniques. Complex **2** has been isolated and characterized in the solid state. Complex **1** undergoes many catalytic cycles without decomposition.

## Experimental Section

**Materials.** Ruthenium chloride was purchased from Johnson Mathey, triphenylphosphine was obtained from Ferak Berling, and $Na_2EDTA$ (AR) was obtained from BDH Chemicals. All organic solvents (AR) used were obtained from BDH and were purified by known methods[32] prior to use. Argon was used without purification. Nitrogen was purified by passing it through vanadous sulfate and alkaline pyrogallate solution and was passed over ascarite before bubbling through the experimental solution. Ruthenium chloride solution was prepared in 1 M hydrochloric acid and estimated spectrophotometrically by the thiourea method[33] and was used after 1 week. The excess of acid in ruthenium(III) solution, which consists of mostly $[RuCl_2(H_2O)_4]^+$ species,[34] was determined by titration of equimolar solution of Ru(III) and EDTA against carbonate-free NaOH. The volume of base consumed by excess acid was subtracted in all the experiments. Elemental analysis were carried out by Amdel, Port Melbourne, Victoria, Australia. IR and far-IR spectra were recorded as Nujol mulls on a Nicolet 200SX FT-IR spectrometer operating under vacuum. $^1H$ and $^{31}P$ NMR spectra were recorded on a JEOL FX100 NMR spectrometer with $Me_4Si$ and 85% phosphoric acid, respectively as standards.

**Synthesis of $[Ru(EDTA\text{-}H)(PPh_3)]$.** A 0.50-g (1-mmol) sample of the complex $K[Ru(EDTA\text{-}H)Cl]\cdot 2H_2O$ prepared by a known procedure[35] was dissolved in water and refluxed in an argon atmosphere for 30–40 min. To this refluxing solution was slowly added triphenylphosphine (0.26 g, 1 mmol) dissolved in a minimum amount of 1,4-dioxane. The mixture was refluxed for a period of 4–6 h until the color of the solution changed from yellow to orange-yellow. The solution was then allowed to cool down when an orange-yellow precipitate settled out. The precipitate was filtered, washed with cold water several times and finally with ether, and dried under vacuo. Yield: 89%.

**Elemental Analysis Data.** Found (calcd): C, 51.04 (51.53); H, 4.83 (4.33); N, 3.91 (4.29). Far-IR: $\nu$(Ru–P) 532 $cm^{-1}$. $^1H$ NMR: phenyl protons at 7.61 ppm (multiplet), $CH_2$ protons at 2.79 ppm (multiplet). $^{31}P\{^1H\}$ NMR: 25.79 ppm (singlet). The complex is paramagnetic, the paramagnetism as determined by the Evans method (1.7 $\mu_B$) corresponds to one unpaired spin for a spin-paired Ru(III) complex.

**Spectrophotometry.** A Beckman Model DU-7 high-speed spectrometer was used to record the spectra and absorbance. Solutions were taken in matched 10-mm quartz cuvettes. All measurements were done at 25 °C, $\mu$ = 0.10 (KCl), and pH 3.00. The pH selected was such that complex formation was maximum in 1:1 Ru(III)–EDTA system.

**Electrochemical Studies.** The electrochemical measurements were made with a Princeton Applied Research (PAR) electrochemical instrument equipped with a precision X-Y recorder. A PAR 174A polarographic analyzer was used to record dc and differential-pulse polarograms (DPP). A PAR 175 universal programmer coupled with a PAR 174A instrument was used for recording cyclic voltammograms (CV). A PAR 303 SMDE assembly provided with DME/HMDE working electrode and Pt wire (0.5 mm diameter) was used. All potentials were measured against a Ag/AgCl reference electrode at 25 °C. A medium-sized drop (2.75 mg mass) was used with an open circuit and a 2 s drop time.

**Potentiometry.** Potentiometric titrations were carried out in a jacketed glass cell through which water at constant temperature was circulated.

---

(6) Groves, J. T.; Nemo, T. E. *J. Am. Chem. Soc.* **1983**, *105*, 5786.

(7) Groves, J. T.; Nemo, T. E. *J. Am. Chem. Soc.* **1983**, *105*, 6243.

(8) Traylor, P. S.; Dolphin, D.; Traylor, T. G. *J. Chem. Soc., Chem. Commun.* **1984**, 279.

(9) Traylor, T. G.; Marsters, J. C., Jr.; Nakano, T.; Dunlap, B. E. *J. Am. Chem. Soc.* **1985**, *107*, 5537.

(10) Lindsay, Smith, J. R.; Mortimer, D. N. *J. Chem. Soc., Chem. Commun.* **1985**, 410.

(11) Groves, J. T.; Hanshalter, R. C.; Nakamura, M.; Nemo, T. E.; Evans, B. J. *J. Am. Chem. Soc.* **1981**, *103*, 2884.

(12) (a) Nee, M. W.; Bruice, T. C. *J. Am. Chem. Soc.* **1982**, *104*, 6123. (b) Bruice, T. C.; Chi, Y. L. *J. Am. Chem. Soc.* **1985**, *107*, 512.

(13) LaMar, G. N.; DeRopp, J. S.; Latos Grazynski, L.; Balch, A. L.; Johnson, R. B.; Smith, K. M.; Paresh, D. W.; Ching R.-J. *J. Am. Chem. Soc.* **1983**, *105*, 782.

(14) Smegal, J. A.; Schardt, B. C.; Hill, C. L. *J. Am. Chem. Soc.* **1983**, *105*, 3510.

(15) Groves, J. T.; Kruper, W. J., Jr.; Hanshalter, R. C. *J. Am. Chem. Soc.* **1980**, *102*, 6375.

(16) Ehrenfeld, G. M.; Murugasen, N.; Hecht, S. M. *Inorg. Chem.* **1984**, *23*, 1496.

(17) Murugasen, N.; Hecht, S. M. *J. Am. Chem. Soc.* **1985**, *107*, 493.

(18) Frankline, C. C.; Van Aita, R. B.; Tai, A. F.; Valentine, J. S. *J. Am. Chem. Soc.* **1984**, *106*, 814.

(19) Van Aita, R. B.; Franklin, C. C.; Valentine, J. S. *Inorg. Chem.* **1984**, *23*, 4121.

(20) Collman, J. P.; Kodadek, T.; Raybuck, S. A.; Brauman, J. I.; Papazian, L. M. *J. Am. Chem. Soc.* **1985**, *107*, 4343.

(21) Collman, J. P.; Brauman, J. I.; Meunier, B.; Hayashi, T.; Kodadek, T.; Raybuck, S. A. *J. Am. Chem. Soc.*, **1985**, *107*, 2000.

(22) Moyer, B. A.; Keithsipe, B.; Meyer, T. J. *Inorg. Chem.* **1981**, *20*, 1475.

(23) James, B. R.; Mikkel Sen, S. R.; Leung, T. W.; Williams, G. M.; Wong, R. *Inorg. Chim. Acta* **1984**, *85*, 209.

(24) Berg, J. M.; Holm, R. H. *J. Am. Chem. Soc.* **1985**, *107*, 917.

(25) Graham, B. W.; Laing, K. R.; O'Connor, C. J.; Roper, W. R. *J. Chem. Soc. D* **1970**, 1272.

(26) Graham, B. W.; Laing, K. R.; O'Connor, C. J.; Roper, W. R. *J. Chem. Soc., Dalton Trans.* **1972**, 1237.

(27) Sen, A.; Halpern, J. *J. Am. Chem. Soc.* **1977**, *99*, 8337.

(28) Hanzlik, R. P.; Williamson, D. *J. Am. Chem. Soc.* **1976**, *98*, 6570.

(29) Chen, G. J. J.; McDonald, J. W.; Newton, W. E. *Inorg. Chem.* **1976**, *15*, 2612.

(30) Groves, J. T.; Quinn, R. *J. Am. Chem. Soc.* **1985**, *107*, 5790; *Inorg. Chem.* **1984**, *23*, 3846.

(31) Taqui Khan, M. M. *Proceeding of the 4th International Conference on Homogeneous Catalysis, Leningrad, USSR, Sept 1984*, Gordon & Breach: New York; in press.

(32) Vogel, A. I. *Textbook of Practical Organic Chemistry*, Longman: Birmingham, AL, 1976.

(33) Arey, G. H.; Young, F. *Anal. Chem.* **1950**, *22*, 1277.

(34) Taqui Khan, M. M.; Ramachandraiah, G.; Prakash Rao, A. *Inorg. Chem.* **1986**, *25*, 665.

(35) Diamantis, A. A.; Dubrawski, J. V. *Inorg. Chem.* **1981**, *20*, 1142.

**Table I.** Equilibrium Data for 1:1 Ru(III)–EDTA and 1:1:1 Ru(III)–EDTA–$PPh_3$ Systems in a Water–Dioxane (1:1) Medium in the Presence of Nitrogen and Oxygen at 35 °C and $\mu = 0.10$ M (KCl)

| const | equilibrium quotient | potentiometry[a] | spectrophotometry[a,b] |
|---|---|---|---|
| $\log K_a$ | $[HL][H^+]/[H_2L]$ | −6.80 | |
| $\log K_{2a}$ | $[L][H^+]/[HL]$ | −9.90 | |
| $\log K_1$ | $[ML]/[M][L]$ | 15.34 | 15.25 |
| $\log \beta^{O_2}{}_{22}$ | $[M_2L_2O_2(OH)][H^+]/[M]^2[L]^2$ | 30.40 | 29.02 |
| $\log \beta_{11}$ | $[MLA]/[M][L][A]$ | | 17.31 |
| $\log \beta^{O_2}{}_{222}$ | $[(MLA)_2]/[M]^2[L]^2[A]^2$ | | 33.17 |
| $\log K^{OH}{}_1$ | $[MLOH][H^+]/[ML]$ | −3.20 | |
| $\log K_2{}^c$ | $[[LRu^{IV}(PPh_3)]_2O_2]/$<br>$[LRu(III)(PPh_3)]^2$ | 3.62 | |
| $\log K_{11}$ | $[MLA]/[ML][A]$ | | 2.06 |

[a] The constants are accurate to ±0.04. [b] At 25 °C and pH 3.00. [c] Determined kinetically at 35 °C.

Nitrogen, purified by passing through vanadous sulphate and alkaline pyrogallate, was continuously bubbled during titration. For the titrations under oxygen the gas passed over ascarite was bubbled during the titration.

The method consisted of titration of EDTA in the absence and in presence of 1 equiv of Ru(III) against carbonate-free sodium hydroxide. All the titrations were performed at 35 °C and $\mu = 0.10$ (KCl) in a 50% (v/v) water–dioxane medium.

A Digisun Model DI-707 pH meter correct to 0.01 pH fitted with a combination glass electrode was used to measure $-\log\,[H^+]$. The electrode system was calibrated below pH 3.50 by titration of HCl in aqueous and 50% water–dioxane media and comparing pH in both media. Similarly for calibration of pH in the basic range NaOH was added in small amounts and pH noted in aqueous and 50% water–dioxane media.

**Kinetic Studies.** The reactions were carried out in a 1:1 water–dioxane mixture. The rate of absorption of oxygen was measured by using a glass manometric apparatus provided with leak-proof springham stopcocks. High-vacuum silicon grease was applied to the stopcocks to keep the system air-tight. The temperature of the reaction was maintained constant by circulating water at a particular temperature through a jacketed glass cell. The standard pressure of oxygen employed was 0.2–1 atm.

The disodium salt of ethylenediaminetetraacetic acid was dissolved in water. The Ru(III)–EDTA complex was prepared in the reaction mixture by adding the solutions of $RuCl_3$ and EDTA in a 1:1 ratio. The pH of the solution was maintained at 3.00 by adding carbonate-free NaOH solution.

The system was evacuated and flushed with oxygen several times to ensure that a complete oxygen atmosphere prevails in the reaction cell. Sufficient time was given for the solution to attain equilibrium. Triphenylphosphine was dissolved in sufficient quantity of dioxane to maintain a 1:1 water–dioxane ratio in the reaction mixture. In order to minimize the effect of solvent vapor, a blank was run simultaneously under the same conditions of temperature, pressure, and volume. The absorption of oxygen was measured manometrically by noting the change in the levels of the indicator solution in the measuring burette at suitable intervals of time. The stirrer was operated at the gas–liquid interface in such a manner that the rate of dissolution of gas was much faster than the rate of absorption by the catalyst and there was no limitation due to diffusion control. It was assumed that Henry's law is obeyed by the system. The catalyst concentration was in the range (0.25–1) × $10^{-4}$ M, the concentration of $PPh_3$ was 1 × $10^{-4}$ to 1 × $10^{-3}$ M, and the oxygen pressure was in the range 0.2–1 atm. All the kinetic measurements were done at 308 K ($\mu = 0.1$ M (KCl)).

## Results

**Potentiometry.** The free-ligand titration curve of EDTA in 50% water–dioxane is presented in Figure 1a. The titration curve shows an inflection at $a = 1$, indicating dissociation of protons from EDTA in separate steps. The dissociation constants were calculated by a known algebraic method[36] and are reported in Table I.

The potentiometric titration curve of Ru(III) and EDTA in a 1:1 ratio under $N_2$ in 50% water–dioxane is presented in Figure 1b. Unlike the 1:1 Ru(III)–EDTA system in water,[37,38] the curve does not show any inflection. The buffer region continues up to $a = 3.0$, beyond which precipitation occurs. This indicates the release of three protons from EDTA in overlapping steps. An extra proton dissociation can be accounted for by considering a 1:1 chelate formation and subsequent hydrolysis of the chelate according to the following reactions:

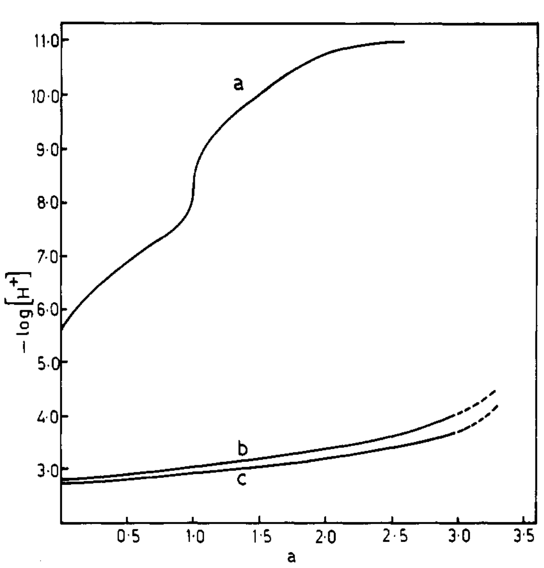

**Figure 1.** Potentiometric titration curves of (a) the free ligand, (b) the 1:1 Ru(III)–EDTA system under $N_2$, and (c) the 1:1 Ru(III)–EDTA system under $O_2$, in 50% water–dioxane medium. $t = 35$ °C; $\mu = 0.10$ M (KCl).

$$M + L \underset{}{\overset{K_1}{\rightleftharpoons}} ML \qquad K_1 = [ML]/[M][L] \tag{1}$$

$$\begin{gathered} ML \overset{K^{OH}{}_1}{\rightleftharpoons} MLOH + H^+ \\ K^{OH}{}_1 = [MLOH][H^+]/[ML] \end{gathered} \tag{2}$$

(where L = $EDTA^{4-}$, the charges are omitted on the species for the sake of clarity). The constants $K_1$ and $K^{OH}{}_1$ calculated by an algebraic method and refined by successive approximations are presented in Table I.

The potentiometric titration curve of 1:1 Ru(III)–EDTA under oxygen in 50% water–dioxane is presented in Figure 1c. The titration curve under $O_2$, like the corresponding curve under $N_2$, does not show any inflection. The buffer region continues up to $a = 3.0$, where precipitation starts. The titration curve under oxygen, however, lies at a lower pH than the curve under nitrogen, indicating interaction of dioxygen with Ru(III)–EDTA in solution. Interaction of dioxygen with the complex commences from $a = 0$ onward as shown by the lowering of the titration curve under oxygen as compared to the curve under nitrogen. The following reaction was assumed to take place under oxygen between $a =$ 0–2.5:

$$\begin{gathered} 2M + 2L \overset{\beta^{O_2}{}_{22}}{\rightleftharpoons} M_2L_2O_2(OH) + H^+ \\ \beta^{O_2}{}_{22} = [M_2L_2O_2(OH)][H^+]/[M]^2[L]^2 \end{gathered} \tag{3}$$

Since precipitation takes place at $a > 3.0$, the hydrolysis constant could not be calculated. The constant $\beta^{O_2}{}_{22}$ calculated by an algebraic method is presented in Table I.

**Spectrophotometry.** Triphenylphosphine ($PPh_3$) does not have a titratable proton. For this reason the potentiometric titration of 1:1:1 Ru(III)–EDTA–$PPh_3$ system under nitrogen and oxygen could not be done. Instead, a spectrophotometric method was used to determine the mixed-ligand formation constants of these systems.

The absorption spectrum of 1:10 Ru(III)–EDTA solution under nitrogen showed bands at 217, 246, 316, 368 and 486 nm. The band at 486 nm was sensitive to changes to the environment of the metal ion in all the systems studied. Therefore, this peak was

---

(36) Taqui Khan, M. M.; Amjad Hussain. *Ind. J. Chem., Sect. A* **1980**, *19A*, 50.

(37) Taqui Khan, M. M.; Ramachandraiah, G. *Inorg. Chem.* **1982**, *21*, 2109.

(38) Taqui Khan, M. M. *Pure Appl. Chem.* **1983**, *35*, 159.

**Table II.** Electronic Absorption Spectral Data for the 1:1 Ru(III)-EDTA and 1:1:1 Ru(III)-EDTA-PPh$_3$ Systems at pH 3.00, $t$ = 25 °C, and $\mu$ = 0.10 M (KCl)

| complex | $\lambda_{max}$, nm ($\epsilon$, cm$^{-1}$ mol$^{-1}$ dm$^3$) | |
|---|---|---|
| | $N_2$ | $O_2$ |
| RuCl$_3$ | 555 (4.5 × 10$^2$) | 555 (4.5 × 10$^2$) |
| | 487 (5.9 × 10$^2$) | 487 (5.9 × 10$^2$) |
| | 296 (2.8 × 10$^3$) | 296 (2.8 × 10$^3$) |
| | 247 (4.3 × 10$^3$) | 247 (4.3 × 10$^3$) |
| | 217 (3.1 × 10$^3$) | 217 (3.1 × 10$^3$) |
| Ru(III)-EDTA | 484 (6.1 × 10$^2$) | 486 (2.5 × 10$^2$) |
| | 368 (1.9 × 10$^3$) | 390 (8.5 × 10$^2$) |
| | 316 (2.7 × 10$^3$) | 311 (2.7 × 10$^3$) |
| | 246 (4.1 × 10$^3$) | 241 (3.8 × 10$^3$) |
| | 217 (3.1 × 10$^3$) | 217 (3.1 × 10$^3$) |
| Ru(III)-EDTA-PPh$_3$ | 485 (3.8 × 10$^2$) | 636 (10) |
| | 375 (1.6 × 10$^3$) | 487 (6.3 × 10$^2$) |
| | 316 (2.8 × 10$^3$) | 390 (1.9 × 10$^3$) |
| | 260 (6.7 × 10$^3$) | 316 (2.8 × 10$^3$) |
| | 217 (3.1 × 10$^3$) | 260 (1.1 × 10$^4$) |
| | | 217 (3.1 × 10$^3$) |

used as the characteristic ($\lambda_{max}$) for the Ru(III)-EDTA complex for the determination of the formation constant. In the presence of a tenfold excess of the ligand the equilibrium for the formation of Ru(III)-EDTA complex shifts toward the right, and the absorbance will essentially be due to the 1:1 complex. Thus extinction coefficient of the complex at the $\lambda_{max}$ value of 486 nm can be calculated by the Beer's law relationship

$$A = \epsilon C l \tag{4}$$

where $A$ = absorbance, $\epsilon$ = extinction coefficient, $C$ = concentration of complex, and $l$ = pathlength of the cell. $\epsilon$ at $\lambda_{max}{}^{486}$ was found to be 707.5.

For the 1:1 Ru(III)-EDTA system under nitrogen in 50% water-dioxane the following equilibrium was considered:

$$M + L \overset{K_1}{\rightleftharpoons} ML \tag{5}$$

From the necessary material balance equations, the constant $K_1$ was calculated and tabulated in Table I. The value log $K_1$ = 15.25 agrees very well with the value of 15.34 obtained potentiometrically.

In the case of Ru(III)-EDTA system under oxygen in the mixed-solvent system, the following equilibrium was considered at pH 3.00:

$$2M + 2L + H_2O \underset{O_2}{\overset{\beta^{O_2}{}_{22}}{\rightleftharpoons}} (ML)_2(OH)(O_2) + H^+ \tag{6}$$

The constant $\beta^{O_2}{}_{22}$ was calculated by setting up appropriate material balance equations, and the calculated value is reported in Table I. The value agrees very well with that obtained potentiometrically.

For the 1:1:1 Ru(III)-EDTA-PPh$_3$ system under nitrogen in 50% water-dioxane the following equilibrium was considered:

$$M + L + A \overset{\beta_{11}}{\rightleftharpoons} MLA \qquad \beta_{11} = [MLA]/[M][L][A] \tag{7}$$

$$L = EDTA^{4-},\ A = PPh_3$$

$\beta^{11}$ was calculated from the appropriate material balance equations and tabulated in Table I.

The absorption of Ru(III)-EDTA-PPh$_3$ system under oxygen shows a new band at 390 nm, which is characteristic of the dioxygen complex.[28] This indicates the formation of a dioxygen complex according to the following equilibrium:

$$\begin{gathered} 2M + 2L + 2A \overset{\beta^{O_2}{}_{222}}{\rightleftharpoons} (MLA)_2O_2 \\ \beta^{O_2}{}_{222} = [(MLA)_2O_2]/[M]^2[L]^2[A]^2 \end{gathered} \tag{8}$$

From the appropriate material balance equations the constant $\beta^{O_2}{}_{222}$ was calculated and reported in Table I.

The electronic spectral data of 1:1 Ru(III)-EDTA solutions under nitrogen and oxygen and those of the 1:1:1 Ru(III)-EDTA-PPh$_3$ solutions under nitrogen and oxygen are presented in Table II.

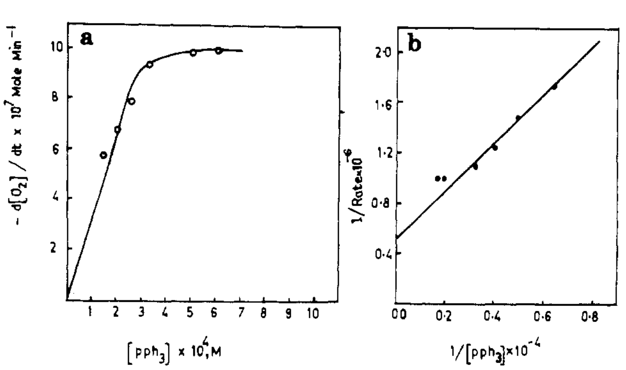

**Figure 2.** (a) Plot of rate vs. [PPh$_3$] at a constant catalyst concentration of 6 × 10$^{-5}$ M at 35 °C, $\mu$ = 0.10 M (KCl), and pH 3.00. (b) Plot of reciprocal rate vs. reciprocal of [PPh$_3$] under the same conditions as part a.

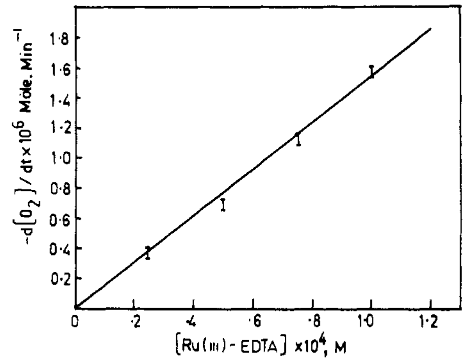

**Figure 3.** Plot of rate observed vs. catalyst concentration at a constant concentration of the substrate of 3 × 10$^{-4}$ M at 35 °C, $\mu$ = 0.10 M (KCl), and pH 3.00.

**Electrochemical Studies.** DPP and CV data of 1:1 Ru(III)-EDTA and 1:1:1 Ru(III)-EDTA-PPh$_3$ systems under nitrogen and oxygen are presented in Table III.

**Kinetics of Oxidation of PPh$_3$.** The oxidation of PPh$_3$ was carried out in a 50% water-dioxane medium at pH 3 and 35 °C. The rate of oxidation was obtained from the tangent of the plot of the number of moles of oxygen absorbed vs. time at constant temperature, oxygen pressure, and catalyst and substrate concentration. Conversion to the rate of oxidation of PPh$_3$ was obtained from the stoichiometric relationship:

$$-d[O_2]/dt = -\tfrac{1}{2}d[PPh_3]/dt$$

**Dependence of the Rate on the PPh$_3$ Concentration.** The plot of the rate of consumption of oxygen as a function of the concentration of PPh$_3$ at constant concentration of catalyst in a Ru(III)-EDTA:PPh$_3$ ratio up to 1:10 is linear, showing first-order dependence (Figure 2a). Saturation kinetics are observed at catalyst:substrate concentration ratios of more than 10, and the rate becomes virtually independent of substrate concentration. A plot of reciprocal of $k_{obsd}$ vs. the reciprocal of the phosphine concentration gives a straight line (Figure 2b).

**Dependence of the Rate on the Catalyst Concentration.** Figure 3 shows a plot of the rate of oxidation of PPh$_3$ at constant [PPh$_3$] as a function of the concentration of the catalyst. The data fits a first-order plot with respect to the catalyst.

**Dependence of the Rate on the Oxygen Concentration.** Figure 4 illustrates the dependence of the rate of oxidation of PPh$_3$ on the oxygen concentration at constant PPh$_3$ and catalyst concentrations. The plot of –log (d[O$_2$]/d$t$) vs. –log[O$_2$] is linear with a slope equal to 0.5, showing a one-half-order dependence with respect to molecular oxygen.

## Discussion

The spectroscopic and electrochemical data on RuCl$_3$ solutions in 1:1 water-dioxan are given in Tables II and III. It was shown

**Table III.** Differential-Pulse Polarographic (DPP) and Cyclic Voltammetric (CV) Data for 1:1 Ru(III)-EDTA and 1:1:1 Ru(III)-EDTA-$PPh_3$ Systems in Water-Dioxane (1:1) at pH 3.00, $t$ = 25 °C, and $\mu$ = 0.10 M (KCl)

| | DPP | | CV | | | |
|---|---|---|---|---|---|---|
| | under $N_2$ | under $O_2$ | under $N_2$ | | under $O_2$ | |
| complex | $-E_{1/2}$, V | $-E_{1/2}$, V | $-E_{pc}$, V | $-E_{pa}$, V | $-E_{pc}$, V | $-E_{pa}$, V |
| $RuCl_3$ | 0.390 | 0.390 | 0.510 | 0.270 | 0.510 | 0.270 |
| | 0.965 | 0.965 | | | | |
| Ru(III)-EDTA | 0.270 | 0.260 | 0.310 | 0.230 | 0.326 | 0.226 |
| | 0.895 | 0.468 | 0.555 | 0.471 | 0.710 | 0.560 |
| | 1.140 | 0.665 | | | | |
| | | 1.100 | | | | |
| Ru(III)-EDTA-$PPh_3$ | 0.170 | 0.070 | 0.245 | 0.215 | 0.100 | 0.070 |
| | 0.878 | 0.285 | | | 0.342 | 0.228 |
| | 1.295 | 0.485 | | | 0.552 | 0.590 |
| | | 0.730 | | | 0.790 | |
| | | 1.140 | | | | |

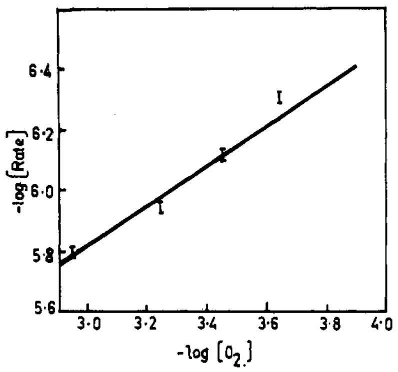

**Figure 4.** Plot of −log rate vs. −log [$O_2$] at a constant catalyst and substrate concentration. Catalyst: substrate ratio = 1:10 at 35 °C, $\mu$ = 0.10 M (KCl), and pH 3.00.

in an earlier communication[34] that the major species of Ru(III) in solution at pH 3.00 is the $[RuCl_2(H_2O)_4]^+$ ion.

As expected, the value of the equilibrium constant log $K_1$ for the formation of the 1:1 Ru(III)-EDTA complex (Table I) is about 2 log $K$ units higher in 50% water-dioxane as compared to aqueous solution.[39] The hydrolysis constant $K^{OH}_1$ is lower than that in water. The electronic absorption spectrum of 1:1 Ru(III)-EDTA solution under nitrogen exhibits characteristic bands for the d-d transitions of Ru(III) at 368 nm ($\epsilon$ = 1881 $M^{-1}$ $cm^{-1}$) and 484 nm ($\epsilon$ = 614 $M^{-1}$ $cm^{-1}$) (Table II). The high-energy bands are the ligational and CT bands of EDTA.

The DPP of the 1:1 Ru(III)-EDTA system under nitrogen (Table III) shows peaks at −0.270, −0.895, and −1.140 V. The peaks at −0.270 and −0.895 V are assigned[39] to the redox couples $Ru^{3+}/Ru^{2+}$ and $Ru^{2+}/Ru^+$, respectively, and the one at −1.140 V is assigned to the redox couple $H^+/^1/_2H_2$. The values of the redox couples for $Ru^{3+}/Ru^{2+}$ and $Ru^{2+}/Ru^+$ agree with those observed for $RuCl_3$ at −0.390 and −0.965 V, respectively.[34] The CV of the solution (Table III) shows redox peaks at $E_{pc}$ = −0.310 and −0.555 V and $E_{pa}$ = −0.230 and −0.471 V, corresponding to $Ru^{3+}/Ru^{2+}$ and $Ru^{2+}/Ru^+$ couples, respectively. The $E_{pc}$ and $E_{pa}$ values observed in Ru(III)chloride solution are at −0.510 and −0.270 V, respectively.

There is a good agreement in the value of the constant $\beta^{O_2}{}_{22}$ corresponding to the formation of the $\mu$-hydroxo-$\mu$-peroxo Ru(IV) complex $[Ru^{IV}(EDTA)]_2(O_2)(OH)$ (**6**) calculated by potentiometry and spectrophotometry. As in the case of log $K_1$ the value of $\beta^{O_2}{}_{22}$ is higher in the mixed-solvent system as compared[26,27] to $H_2O$. The electronic absorption spectrum of the oxygenated Ru(III)-EDTA system shows besides the ligational bands at 217, 246, and 316 nm a new peak at 390 nm (851). On the basis of the assignment in Co(III)-peroxo complexes this peak can be tentatively assigned to the single $1\pi^*(O_2) \rightarrow d\sigma(Ru(IV))$ LMCT transition in the doubly bridged complex **6**.

In the absorption spectrum of the oxygenated solution of Ru(III)-EDTA, the intensity of the peak at 486 nm, corresponding to the d-d transition of Ru(III), decreases in intensity and the peak at 368 nm disappears, indicating the formation of a Ru(IV) dioxygen complex. The DPP of the 1:1 Ru(III)-EDTA solution under oxygen exhibits four peaks at −0.260, −0.468, −0.665 and −1.100 V. While the peaks at −0.260 and −1.100 V correspond to the redox potential of the $Ru^{3+}/Ru^{2+}$ complex and $H^+/^1/_2H_2$, respectively, as for the Ru(III)-EDTA complex under nitrogen, the peaks at −0.468 and −0.665 V are new and correspond to the stepwise one-electron-redox potentials of the coordinated peroxo group.[39] Such characteristic peaks for a coordinated peroxo group were also observed[39] in the DPP of the complex $[Ru^{IV}(EDTA)(OH)]_2O_2$. The CV of the oxygenated solution exhibits new cathodic and anodic peaks at −0.710 and −0.560 V, corresponding to the oxidation of the coordinated peroxo group.

The formation constant log $\beta_{11}$ for the mixed-ligand Ru(III)-EDTA-$PPh_3$ complex is about 2 log $K$ units more stable than the Ru(III)-EDTA complex (log $K_1$) (Table I). The $\pi$-acidity of $PPh_3$ causes all the protons of EDTA to dissociate off even at $a$ = 0; hence, the stability could not be computed by potentiometry. The absorption spectrum of a 1:1:1 solution of Ru(III)-EDTA-$PPh_3$ under nitrogen shows absorption peaks at 485, 375, 316, and 217 nm. Instead of the peak at 246 nm in the Ru(III)-EDTA solution a new peak appeared at 260 nm ($\epsilon$ = 6748 $M^{-1}$ $cm^{-1}$). This peak can be attributed to the LMCT band of the coordinated triphenylphosphine ligand.

The DPP of the 1:1:1 Ru(III)-EDTA-$PPh_3$ solution (Figure 5a) shows peaks corresponding to $Ru^{3+}/Ru^{2+}$ and $Ru^{2+}/Ru^+$ reduction at −0.170 and −0.878 V. The peak corresponding to $Ru^{3+}/Ru^{2+}$ reduction is about 0.1 V more positive than the that of Ru(III)-EDTA solution because of the presence of the $\pi$-acidic $PPh_3$ group. The peak due to $Ru^{2+}/Ru^+$ is about 0.017 V more positive than that for the Ru(III)-EDTA system. The $H^+/^1/_2H_2$ potential at −1.295 V is more negative by about 0.16 V as compared to that for the Ru(III)-EDTA system (Figure 5a). The $E_{1/2}$ values of the $Ru^{3+}/Ru^{2+}$ and $Ru^{2+}/Ru^+$ complexes observed from the CV of the Ru(III)-EDTA-$PPh_3$ solution are more positive[39] than those of the Ru(III)-EDTA solution (Table III).

The DPP of the oxygenated solution of Ru(III)-EDTA-$PPh_3$ (Figure 5b) shows peaks at −0.070 V than can be assigned to the $Ru^{4+}/Ru^{3+}$ couple. Potentials in the range of 0.1-0.2 V were reported[40] for the $Ru^{4+}/Ru^{3+}$ couple in the complex $RuX_2T_2$ (X = Cl, Br; T = 1-alkyl-3-aryltriazene 1-oxide) in acetonitrile medium. The potentials for $Ru^{(n+1)+}/Ru^{n+}$ couples are pH-dependent[41] and become more negative with an increase in pH. The peak corresponding to the $Ru^{3+}/Ru^{2+}$ couple[39] was observed at −0.285 V. The peaks characteristic of the stepwise reduction of the coordinated peroxo group appear at −0.485 and −0.730 V. Corresponding peaks were observed[39] in the CV of $[Ru^{IV}$-

---

[39] Taqui Khan, M. M.; Hussain, A.; Ramachandraiah, G.; Moiz, M. A. *Inorg. Chem.*, in press.

[40] Bhattacharya, S.; Chakravorty, A.; Cotton, F. A.; Mukherjee, R.; Schwotzer, W. *Inorg. Chem.* **1984**, *23*, 1709.

[41] Takeuchi, K. J.; Thompson, M. S.; Pipes, D. W.; Meyer, T. J. *Inorg. Chem.* **1984**, *23*, 1845.

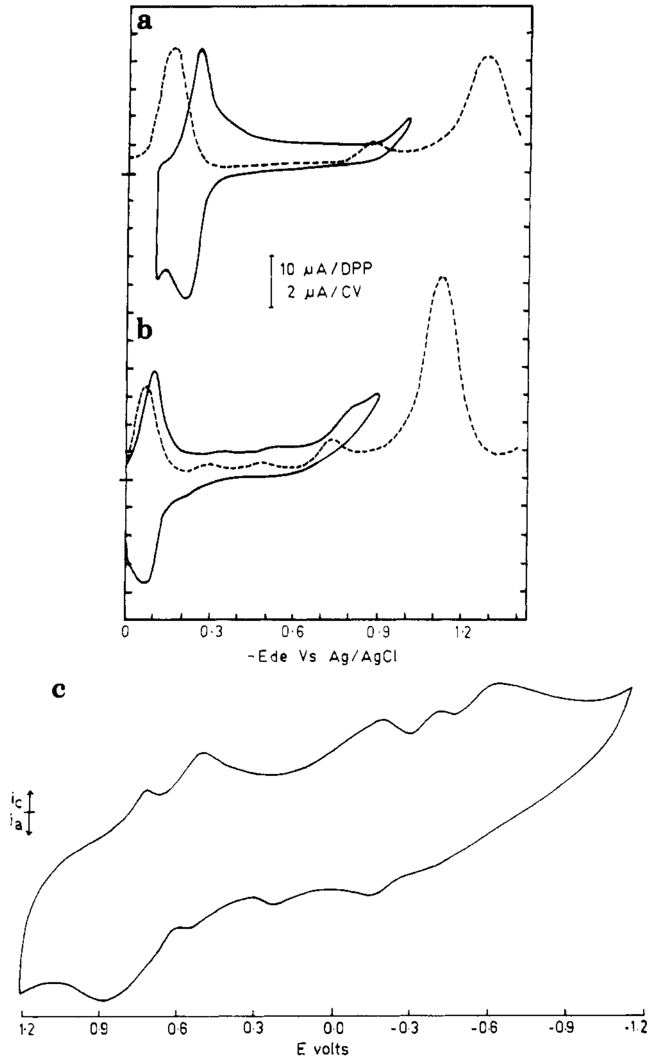

**Figure 5.** (a,b) Differential pulse (- -) and cyclic voltammograms (—) of 1:1:1 Ru(III)-EDTA-$PPh_3$ solution in 50% water-dioxane medium at 25 °C, $\mu$ = 0.10 M (KCl), and pH 3.00: (a) under nitrogen; (b) under oxygen. Part c shows a cyclic voltammogram of a (1 × $10^{-3}$ M) solution of the ruthenyl species [(EDTA-H)$Ru^V$=O], $\mu$ = 0.1 M ($NaClO_4$), with a glassy-carbon working electrode and Ag/AgCl as reference electrode

(EDTA-H)(OH)]$_2O_2$ complex at −0.529 and −0.660 V, respectively. The CV of the solution show cathodic peaks corresponding to the reduction of the coordinated peroxo group at −0.552 and −0.790 V and an anodic peak at −0.590 V (Figure 5b).

Additional evidence for the formation of a [(EDTA)$Ru^V$=O] species in the reaction is provided by the isolation[42] of the solid [(EDTA-H)$Ru^V$=O] complex (**7**) as a stable greenish brown compound by the interaction of iodosylbenzene with the [Ru(EDTA)($H_2O$)]$^-$ complex in aqueous solution. Complex **7** exhibits the $\nu$($Ru^V$=O) stretch at 870 cm$^{-1}$. The CV of the complex in a $HClO_4$-$NaClO_4$ medium at pH 3.00 with a glassy-carbon electrode (Figure 5c) gives $E^{1/2}$ values for $Ru^{5+}/Ru^{4+}$ at +0.77 V, $Ru^{4+}/Ru^{3+}$ at +0.53 V, $Ru^{3+}/Ru^{2+}$ at +0.01 V and $Ru^{2+}/Ru^{+}$ at −0.40 V. A potential of +0.62 V has been reported[43] for $Ru^{4+}/Ru^{3+}$ in the complex [$Ru^{IV}$=O(TMC)($H_2O$)]$^{2+}$ (TMC = 1,4,8,11-tetramethyl-1,4,8,11-tetraazacyclotetradecane) in a solution of *p*-toluenesulfonic acid. The potential was reported[44] to be dependent on pH and scan rate. For the dioxo $Ru^{VI}$ species [$Ru^{VI}(O)_2$(TMC)]$^{2+}$ a combined two-electron potential of +0.66 V was reported[44] for the $Ru^{6+}/Ru^{5+}$ and $Ru^{5+}/Ru^{4+}$ couples, 0.36 V for the $Ru^{4+}/Ru^{3+}$ couple, and 0.15 V for the $Ru^{3+}/Ru^{2+}$ couple. The CV of the complex [Ru(EDTA)($PPh_3$)] with the glassy-carbon electrode shows peaks similar to the Ru(III)-EDTA-$PPh_3$ solution under $N_2$.

**Scheme I**

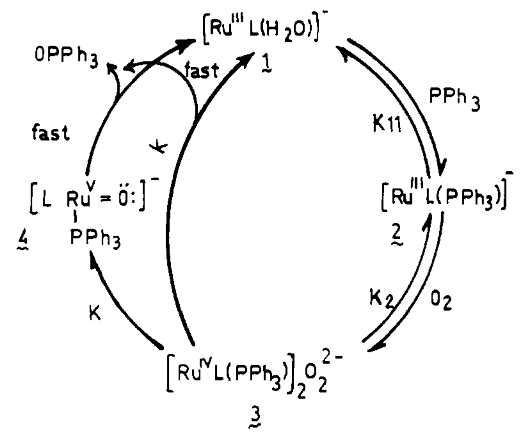

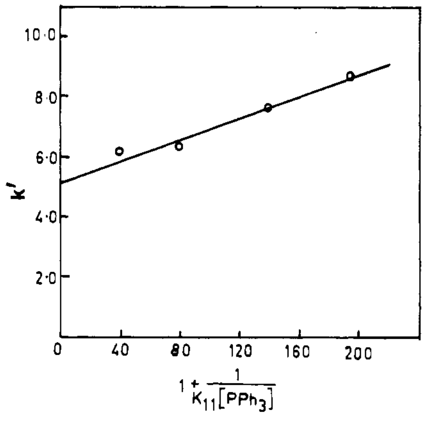

**Figure 6.** Plot of $k'$ vs. 1 + 1/$K_{11}$[$PPh_3$] at 35 °C, $\mu$ = 0.10 M (KCl), and pH 3.00.

The oxygenated solution of Ru(III)-EDTA-$PPh_3$ shows a shoulder at 390 nm ($\epsilon$ = 1.9 × $10^2$ M$^{-1}$ cm$^{-1}$) corresponding either to the $1\pi^*(O_2) \rightarrow d\sigma(Ru^{4+})$ LMCT band of the intermediate peroxo complex [Ru(EDTA)($PPh_3$)]$_2O_2$ or the $^1p\pi(O^{2-}) \rightarrow d\pi(Ru^{4+})$ charge-transfer band in the transient [$Ru^V$=O(EDTA)($PPh_3$)] (**4**) species. A weak absorption band at 390 nm ($\epsilon$ = 550 M$^{-1}$ cm$^{-1}$) was reported[43] for the oxo complex [$Ru^{IV}$=O(TMC)($H_2O$)]$^{2+}$. We have earlier observed[39] the 390-nm band for the complex [Ru(EDTA-H)(OH)]$_2O_2$ (**5**). Whereas the 390-nm band in **5** is an intense peak, it is a shoulder in the oxygenated Ru(III)-EDTA-$PPh_3$ (**3**) solution. It is a coincidence[45] that the ($\mu$-peroxo)cobalt(III) complexes also exhibit a LMCT band for $1\pi^*(O_2) \rightarrow d\sigma(Co^{3+})$ around 390 nm. The bands in the 450–550-nm region in oxygenated Ru(III)-EDTA-$PPh_3$ may be assigned to the d–d transition with LMCT character.

**Mechanism of Triphenylphosphine Oxidation.** The kinetic data pertaining to the oxidation of $PPh_3$ confirm the catalytic cycle shown in Scheme I.

The rate law based on the reaction mechanism proposed in Scheme I under a steady-state concentration of **2** can be written as follows:

$$k' = \frac{[Ru^{III}L]_T[O_2]^{1/2}}{-d[O_2]/dt} = \frac{2}{kK_{11}K_2[PPh_3]} + \frac{2}{kK_2} + \frac{2[O_2]^{1/2}}{k} = \frac{2}{kK_2}\left(1 + \frac{1}{K_{11}[PPh_3]}\right) + \frac{2[O_2]^{1/2}}{k} \qquad (9)$$

L = EDTA

---

[42] Taqui Khan, M. M.; Abdi, S. H. R. *J. Chem. Soc., Chem. Commun.*, in press.

[43] Che, C. M.; Tang, T. W.; Poon, C.-K. *J. Chem. Soc., Chem. Commun.* **1984**, 641.

[44] Che, C. M.; Wong., K.-Y.; Poon, C.-K. *Inorg. Chem.* **1985**, *24*, 1797.

[45] Riley, D. P. *Inorg. Chem. Acta* **1985**, *99*, 5.

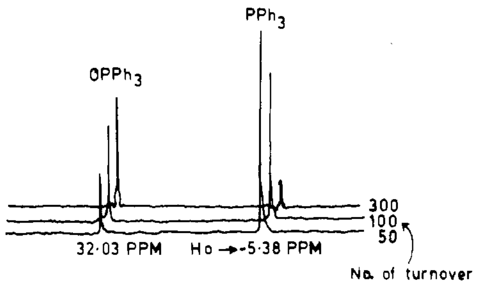

**Figure 7.** $^{31}P\{^1H\}$ NMR spectra of $PPh_3$ and $OPPh_3$ at different turnover numbers.

Here $K_{11}$ and $K_2$ are preequilibrium steps and $k$ is the rate-determining step. The plot of $k'$ vs. $1 + 1/K_{11}[PPh_3]$ gives a straight line (Figure 6) with a slope equal to $2/kK_2$ and intercept equal to $2[O_2]^{1/2}/k$. From the values of the slope and intercept of Figure 6, the value of rate constant $k$ and the equilibrium constant $K_2$ at 35 °C ($\mu = 0.1$) have been calculated as $1.3 \times 10^{-2}$ $min^{-1}$ and $4.26 \times 10^3$ $M^{-1}$, respectively. The value of $K_{11}$ calculated spectrophotometrically is presented in Table I.

In the proposed mechanism (Scheme I) the Ru(III)–EDTA complex (**1**) reacts with triphenylphosphine in the preequilibrium step $K_{11}$ to form a mixed-ligand Ru(III)–EDTA–$PPh_3$ complex (**2**). The formation of complex **2** has been confirmed by potentiometric and spectrophotometric methods and also by the isolation of the complex in the solid state.

Complex **2** reacts with $O_2$ to form the $\mu$-peroxo–Ru(IV) species **3**. The formation of **3** is confirmed on the basis of kinetic data (dependence of the rate on oxygen concentration) and the appearance of the characteristic CT band at 390 nm in the absorption spectrum of the complex. The DPP and CV of the oxygenated (1:1:1) Ru(III)–EDTA–$PPh_3$ system gives peaks similar to those observed[37,38] in the complex $[Ru^{IV}(EDTA)(OH)]_2O_2$ (**5**), indicating the formation of the $\mu$-peroxo species. The 1:1:1 Ru(III)–EDTA–$PPh_3$ system is stable for a long time under oxygen but in the presence of an excess of $PPh_3$ species **3** changes to the transient species **4**. The rate determining step of the reaction has been proposed as the change of **3** to **4**. The oxygen atom transfer from **3** to $PPh_3$ may be a concerted process with the slow release of the product[20] $OPPh_3$ as rate determining (Scheme I). The two processes cannot however be distinguished on the basis of the rate data available. A supporting evidence for the $[Ru^V{=}O(EDTA)(PPh_3)]$ (**4**) path is the isolation of the parent complex $[Ru^V{=}O(EDTA)]$ (**7**). In the presence of excess of $PPh_3$ however the buildup of **6** from **4** and its subsequent conversion to **3** may be a slow concerted process with steady-state levels of both **6** and **4** in solution.

The buildup of species **4** in the system is expected to be only to the level of steady-state concentration. This is supported by the fact that the same rate constant $k$ was obtained by following the oxidation of $PPh_3$ by the disappearance of the oxo peak at 390 nm and by $^{31}P$ NMR, which shows two peaks initially at −5.38 and 32.03 ppm, corresponding to $PPh_3$ and $OPPh_3$, respectively. The intensity of the $OPPh_3$ peak increases and that of the peak at −5.38 ppm decreases with time and finally disappears when $OPPh_3$ is completely formed ($\alpha$ time). The plots of Figure 7 were used to calculate $k$, which agrees within 1% to the rate constant $1.35 \times 10^{-2}$ $min^{-1}$ determined by oxygen absorption kinetics. Such a behavior was also reported by Holm et al.[24] in the oxidation of $PPh_3$ by $MoO_2(L)$ species (L = 2,6-bis(2,2-diphenyl-2-mercaptoethyl)pyridine), where a steady-state concentration of the molybdyl species is maintained in the system by $R_2SO$.

One of the salient features of the present catalytic system involving the Ru(III)–EDTA–$PPh_3$ system is the completely catalytic nature of the oxygen atom transfer reaction involving dioxygen as the oxidant without the final destruction of the catalyst. The catalytic system Ru(III)–EDTA–$PPh_3$ gives a satisfactory turnover number[46] of 300 mol of $PPh_3$ oxidized/mol of the catalyst. As mentioned earlier, catalytic cycles with $Fe^{IV}{=}O$ system involve iodosylbenzene or peroxy acids as the oxidants.[4-17] The oxidation of $PPh_3$ by the $Ru^{II}(OEP)(PPh_3)$ system was reported[23] to proceed either with the complete decomposition of the complex to form $RuO_2$ and HOEP or by a free-radical outer-sphere oxidation of $PPh_3$. An outer-sphere oxidation of thioethers to sulfoxides by molecular oxygen by *trans*-$RuBr_2(Me_2SO)_4$ was reported by Riley.[45] In this reaction the oxidant is $HO_2^-$. The oxidation of $PPh_3$ by the $PtO_2$ system was also reported[27] to proceed by the nucleophilic displacement of $H_2O_2$ by $PPh_3$ and an outer-sphere oxidation of $PPh_3$ to $OPPh_3$ by $H_2O_2$. The Pt(IV) system is reduced back to Pt(III) by $PPh_3/OH^-$.

Dimerization[28,29] of the catalyst to an inactive product in the catalysis of $MoO_2L_2$ and the destruction of a large amount of the catalyst in the recently reported[30] catalytic system $Ru(TMP)(O_2)$ are some of the difficulties encountered in the complete recycling of the catalyst. The present system Ru(III)–EDTA seems to be an efficient oxygen atom transfer catalytic system where catalysis proceeds with a good turnover number of the product without the loss of the catalyst. The catalytic system offers good promise for the oxidation of olefins to epoxide and alkanes to hydroxy compounds by molecular oxygen. Such studies are now actively in progress.

**Registry No.** $1^-$, 68122-22-5; **2**, 102575-56-4; $3^{2-}$, 102575-57-5; $[(EDTA\text{-}H)Ru^V{=}O]$, 102575-58-6; $PPh_3$, 603-35-0; K[Ru(EDTA-H)-Cl], 14741-19-6; $O_2$, 7782-44-7.

---

(46) turnover number = (yield/100)$[O_2]$/[Ru(III)–EDTA–$PPh_3$].

(47) The periodic group notation in parentheses is in accord with recent actions by IUPAC and ACS nomenclature committees. A and B notation is eliminated because of wide confusion. Groups IA and IIA become groups 1 and 2. The d-transition elements comprise groups 3 through 12, and the p-block elements comprise groups 13 through 18. (Note that the former Roman number designation is preserved in the last digit of the new numbering: e.g., III → 3 and 13.)